Possibility of Gait Analysis with MediaPipe and Its Application in Evaluating the Effects of Gait-assist Devices

Yasutaka Uchida
Dept. of Life Science
Teikyo University of Science
Adachi-ku, Tokyo, Japan
e-mail: uchida@ntu.ac.jp

Tomoko Funayama
Dept. of Occupational therapy
Teikyo University of Science
Uenohara-shi, Yamanashi, Japan
e-mail: funayama@ntu.ac.jp

Yoshiaki Kogure
Professor Emeritus
Teikyo University of Science
Adachi-ku, Tokyo, Japan
e-mail: kogure@ntu.ac.jp

Abstract—**The use of free software in motion analyses in the medical and healthcare fields could contribute to the collection of improved data through rehabilitation and daily health management. The possibility of gait analyses using moving images is examined using the free software, MediaPipe. As a preliminary experiment for applying this software in the rehabilitation field, we attempt a timed up-and-go test and obtain detailed ankle trajectories. Additionally, considering the limitations of the camera installation during measurement, we examine the differences in the camera position when capturing the gait characteristics. Consequently, the characteristics captured were almost similar, although some discrepancies were observed between the data from the front and oblique directions. The detection of the ankle angle was possible. However, a motion analysis using the gait velocity will be required for the correct placement of objects. We analyzed the data obtained from the application of the Orthobot, a gait aid device, for the measurement of gait. The detection of the differences in gait before and after the application of the Orthobot would significantly contribute to the gait assessment. The data were compared with those obtained using ORPHE ANALYTICS. Because MediaPipe only provides relative coordinate values for 33 different target body parts, data interpretation requires correction. However, it proved to be a tool that provided a lot of information by allowing researchers to incorporate the necessary formulas.**

Keywords-Gait analysis; MediaPipe; detection of ankle angle; health care; walking aid device.

I. INTRODUCTION

The measurement of the lower limb function is useful in assisting the prevention of falls. To date, medical and welfare professionals such as rehabilitation and nursing care staff have been responsible for providing support to prevent falls. In recent years, devices for measuring the lower limb function have become widespread. However, the equipment used in rehabilitation medicine and sports requires detailed data and specialized knowledge of the equipment operations. Decisions related to health conditions in daily life are difficult to make. Lower limb dysfunction can lead to serious accidents, such as falls. Stumbling and falling accidents are common social issues [1]–[8].

Wearable devices are now applied in daily life. They can collect various information, such as a runner's running route and speed, as well as their pulse rate. This information can be used as management records by connecting it to the Internet. Daily health-related data managed by servers can be very useful for the elderly. Internet of Things (IoT) devices have been developed for many applications. An IoT device can help prevent falls and stumbling by measuring the ankle joint data. Previously, we measured the gait of hemodialysis patients; however, the analysis required specialized knowledge of machine learning [9]–[12].

MediaPipe is a free software from Google. Numerical data related to faces can be obtained using this software, which specializes in facial data and poses corresponding to the entire body. It is also possible to display three-dimensional (3D) skeletons from two-dimensional (2D) detection on a screen. The ability to see images of the skeleton as it is projected onto the physique can be easily implemented in rehabilitation facilities [13]–[17].

This software provides 3D coordinates that increase its effectiveness. Specifically, if the ankle angles can be obtained from images, it could be a promising alternative for determining physical condition changes based on the experience of physical and occupational therapists. Long-term ankle angle data would also be useful for the early

detection of physical condition changes due to illness or other causes.

Image-based video analyses have long been used in rehabilitation and other medical and healthcare fields, such as the joint research field. Despite the ongoing research, it is impossible to state that image analysis is applied in daily rehabilitation support for patients. The demonstration of the application of video analysis in rehabilitation at a low cost, would cause many people to use it [18]–[22].

Therefore, we examined the possibility of gait analysis by video using MediaPipe. Motion analysis using free software could lead to the rapid spread of video analysis in the medical and healthcare fields.

We adopted this software to conduct a basic analysis of how gait changes using Orthobot®, an assistive device for walking that was not considered previously, to determine the extent to which it can be applied in the field of rehabilitation [23].

If the range of motion of the ankle joint is narrow, even in the lower limbs, the toes do not rise, making it is easy to stumble and fall. We inferred that walking involved not only the lower limb functions but also the entire body.

Considering the gait from an inverted pendulum model, an initial experiment was conducted to determine how the effect of wearing the assistive device would manifest and whether the effect would be sustained by examining the change in the neck angle from the direction perpendicular to the center of the body [24][25].

This research was approved by the Ethics Committee of Teikyo University of Science.

II. EXPERIMENTS

The subjects were two men in their 60s and 70s, respectively. The two gait events differed in terms of the ankle restrictions. The supporter restricted the ankle joint motion. For the elderly patient experience set, the subject wore glasses that did not restrict the ankle joint motion.

The corresponding locations of the 33 landmark data locations on the body output by MediaPipe are listed in Table I.

We used arrays with previously reported pressure sensors to compare the accuracy of the comma-separated value (CSV) data obtained from MediaPipe skeletal certification. The resistance of the pressure sensors changed depending on the pressure, ranging from 100 to 1 MΩ. A 1 kΩ resistor was connected in series with this sensor, and the voltage change of the resistor was used as the input signal. Each sensor measured the voltage at 1 kHz. Eight sensors were arranged parallel to the travel direction. The pressure sensor data were transferred to an Arduino Mega 2560 R3 connected to a personal computer. The connection between the sensors and the Arduino is shown in Figure 1.

TABLE I. Pose Landmark of MediaPipe.

Pose Landmark	
0. nose	
1. left_eye_inner	4. right_eye_inner
2. left_eye	5. right_eye
3. left_eye_outer	6. right_eye_outer
7. left_ear	8. right_ear
9. mouth_left	10. mouth_right
11. left_shoulder	12. right_shoulder
13. left_elbow	14. right_elbow
15. left_wrist	16. right_wrist
17. left_pinky	18. right_pinky
19. left_index	20. right_index
21. left_thumb	22. right_thumb
23. left_hip	24._right_hip
25. left_knee	26. right_knee
27. left_ankle	28. right_ankle
29. left_heel	30. right_heel
31. left_foot_index	32. right_foot_index

The output signals of sensor numbers A0–A7 and the distance between each sensor were used to calculate the walking speed.

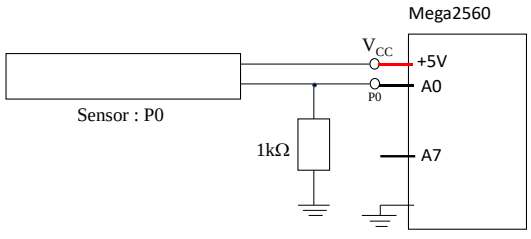

Figure 1. Connection of sensors and Arduino.

A *Accuracy check of CSV data outputed by MediaPipe*

We evaluated the possibility of using CSV data output by MediaPipe to perform gait analysis considering the elderly patient experience set. This measurement indicates the accuracy of the quantification of the ankle position. Because the assessment was performed during gait, we used

images from the timed up-and-go measurement, which is used as a basis for the evaluation of falls experienced by the elderly, to conduct the analysis in MediaPipe.

Figure 2 shows the trajectory of the timed up-and-go measurements. The trajectory was similar to that of the left ankle movement, which was assumed from being seated in the chair to approximately 3 m away and being seated in the chair again. A detailed ankle trajectory was obtained. The video analysis of the timed up-and-go test confirmed the maintenance of the integrity of the specifications [24]–[28].

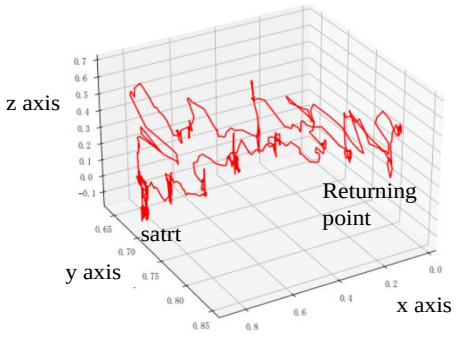

Figure 2. Trajectory of timed up-and-go analyzed by MediaPipe.

B *Results from the front angle*

Gait videos taken from the front under two different conditions, without motion restriction and with motion restricted by a knee supporter, were analyzed using MediaPipe. Figure 3 shows the skeleton analysis of the motion without/with restrictions using a video from the front.

Figure 3. Skeleton analysis of motion (a) without and (b) with restrictions using video from front.

The values of z in Figure 4, which represent the heights of the left and right ankle joints, were plotted against the presence and absence of motion restriction, respectively.

It can be deduced that the time that the heel is on the floor is short because the average of the integrated values of the z values of the foot that applies the restriction is large.

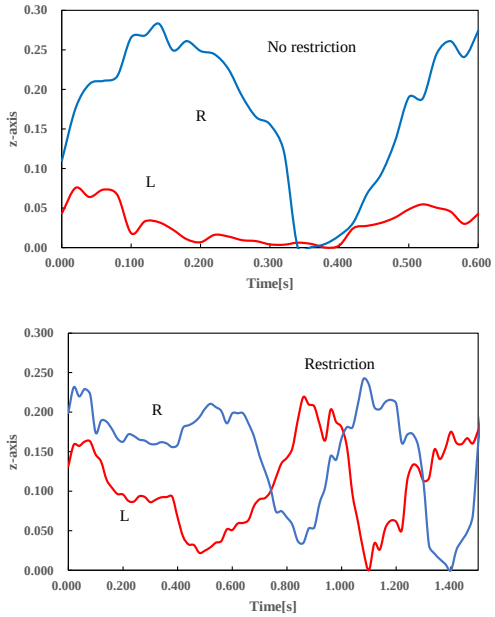

Figure 4. Values of z that represent the ankle height.

C *Results from an oblique upward angle*

In this analysis, the image was obtained from an oblique upward angle to enhance the z-axis length ratio. Peaks corresponding to the left and right toes were also observed. Differences owing to the angle of filming were analyzed from the images obtained from the front and diagonally above the angles.

Figure 5 shows the image without/with restrictions using the video from an oblique angle. The sheet on the floor consisted of the pressure sensors described in Figure 1.

The separately conducted results of the ankle angle measurements indicate that the subjects' left and right feet have different flexibilities. The results are presented in Table II. The left ankle joint was more restricted than the right ankle joint, but there was no significant left-right difference. Therefore, we considered the ankle-to-knee and ankle-to-toe lines as vectors and obtained the angle between them from the inner product. The images were captured in two different ways while the subjects were walking and then analyzed.

Figure 5. Skeleton analysis of motion (a) without and (b) with restrictions using video from oblique upward angle.

TABLE II. Range of Motion.

Direction of motions	R / L Side	Joint angle [deg]
Plantar flexion	R	60
	L	50
Dorsi flexion	R	10
	L	5

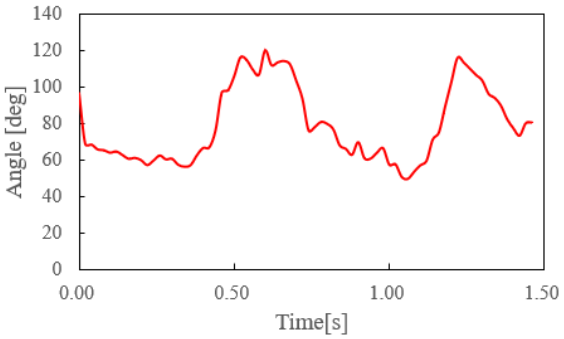

(a)

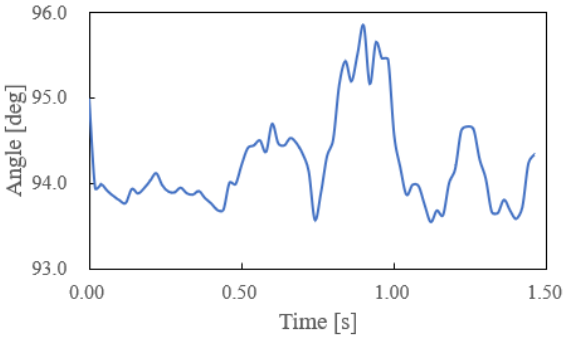

(b)

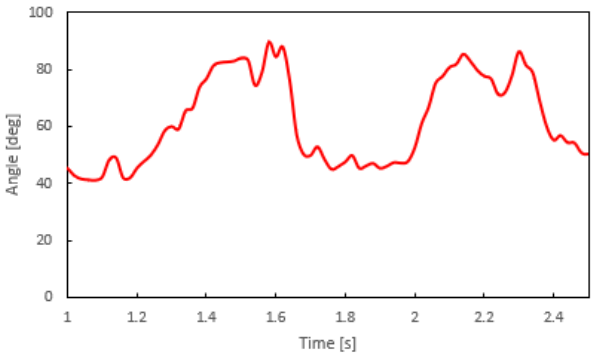

(c)

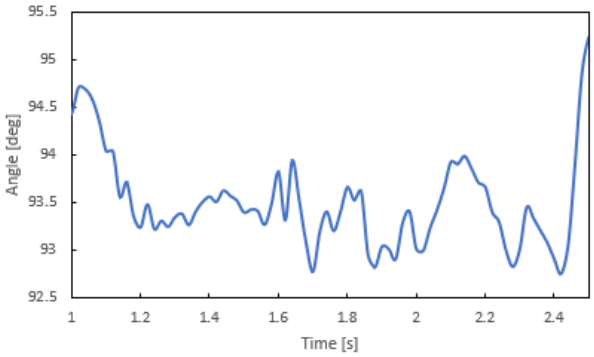

(d)

Figure 6. Results of ankle angle from the front and oblique upward angle

Based on these results, the ankle angles that significantly affected gait were determined. The results of this analysis are shown in Figure 6. The changes in the left and right ankle angles were almost identical with and without motion restriction. However, in both cases, the change in the right ankle angle was smaller. It is unclear whether this was a feature of the subject's gait or a software problem. Further studies with different subjects are necessary to determine the cause.

D Gait speed

The gait speed was examined. Because the coordinates are those of the projection from the camera, correction was required [31]–[34]. Although it is best to correct the coordinates from a 3D viewpoint, in this case, the correction is based on the walking trajectory. Therefore, we compared the walking speeds based on measurements for which specific lengths were known.

For the gait speed, we compared the data from the camera with the data from the pressure sensor and determined the points that should be analyzed to obtain accurate results based on the software. We inferred that it would be difficult to determine the walking speed when shooting from an oblique direction because the screen was moved in an oblique direction. However, data could be

obtained for comparison if the same conditions were used. The problem with the images captured from the front was that the size of the subject varied depending on the measurement data point.

Therefore, we considered the part of the image that moved as slightly as possible on the screen, which was the shoulder area, because it was close to the central part. Figure 7 shows the plot of the right shoulder, which had the largest slope. The obtained value was approximately 0.17, and this value was equal to 0.67 km/h.

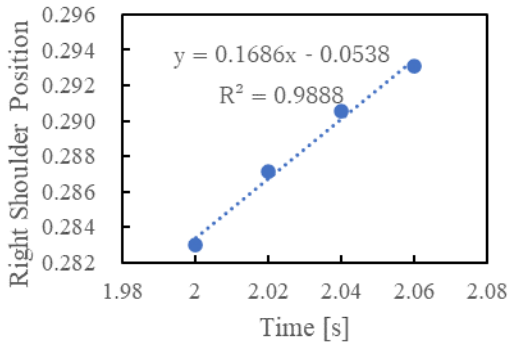

Figure 7. Right shoulder position as a function of time.

Figure 8 shows a 3D display of the trajectory of the right shoulder position. Because the slope of the change in the right shoulder position is approximately 45º, it was deduced that using the correction value for the direction of motion on the screen, a walking speed of 1.4 km/h, which is almost the same as the 1.3 km/h obtained from the mat, could be obtained.

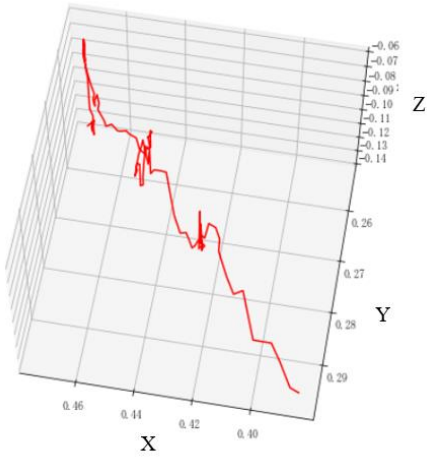

Figure 8. 3D display of the trajectory of the right shoulder position.

E Orthobot

The Orthobot employed in this study is a gait-assist device that supports walking by estimating the gait phase from the thigh posture and generating torque. The Orthobot can be attached to a conventional knee-ankle-foot orthosis to control an individual's knee.

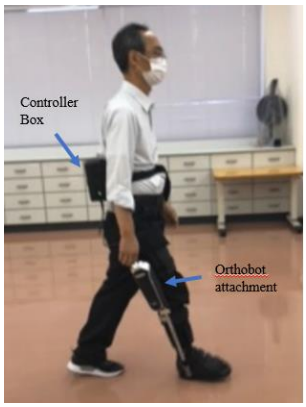

Figure 9. Photograph of the Orthobot attached.

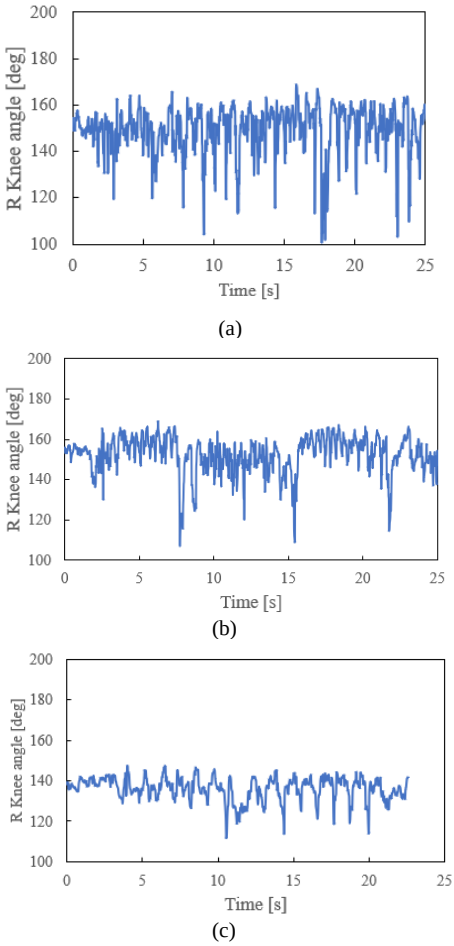

Figure 10. Results of calculated knee angle from MediaPipe.

It automatically assists in the flexion and extension of the knee joint at the appropriate time. The motion state of the leg wearing the aid was measured using drone measurement technology by considering the wearer's swing phase as a pendulum. The torque generated was calculated by estimating the gait phase from the thigh posture to assist walking. Figure 9 shows a photograph of the attached Orthobot.

Orthobots can be attached to general walking aids and are considered highly versatile. The driving device is located in the knee portion, and signals from a controller attached to the back portion of the device move the assistive device, allowing the paralyzed person to experience walking motion, thereby restoring the function.

Figures 10(a)–(c) show the changes in the knee joint during walking before, during, and 5 min after wearing the Orthobot, respectively. The change in the angle of nearly 100° is due to the change in direction. The view of the knee joint angle is not significant during walking, and the machine assists with the swing of the knee. Five minutes after use, the change in the knee joint decreases.

F Neck tilt angle for the subject wearing the walking assist device

Walking affects the entire body and not just the lower extremities. In this section, we focus on the head and neck parts of the body. We used an inverted pendulum model for walking. We calculated how much the neck part was tilted from the axis of the center of the torso during walking, based on the coordinate information obtained from MediaPipe. As shown in Figure 11, the angle of the neck was defined as the angle between the line connecting the coordinates of the midpoints of the left and right shoulders and the coordinates of the midpoints of the left and right hips, and the line connecting the coordinates of the midpoints of the left and right shoulders and the tip of the nose, calculated using the formula for the interior angle of a vector.

The analysis software ORPHE ANALYTICS® manufactured by ORPHE was also used to obtain the neck tilt angle, which was used for confirmation. The neck angle obtained from this software depends on the direction of gait; therefore, absolute values are used because they are positive or negative depending on the gait.

Figure 11. Neck angle definition.

Figure 12 shows the results of the analysis when walking without an aid. It also shows changes in the left and right ankles. The angle of the neck corresponds to the left-side axis, whereas the angles of the left and right heels correspond to the right axis. The measurement started before the movement from the starting point; hence, the walk began facing left approximately 2 s later. At approximately 10 s, the direction changed 180° to a rightward walk. The data started with a leftward walk. At approximately 10 s, the data shows a 180-degree turn around and a rightward walk. Neck movement during walking is in the form of a slowly changing wave with a higher-frequency component. The orange line in the figure shows the left heel change, whereas the gray line shows the right heel. The values are larger at farther distances from the camera. The vertical movement of the heel changed in response to the neck tilt angle signal.

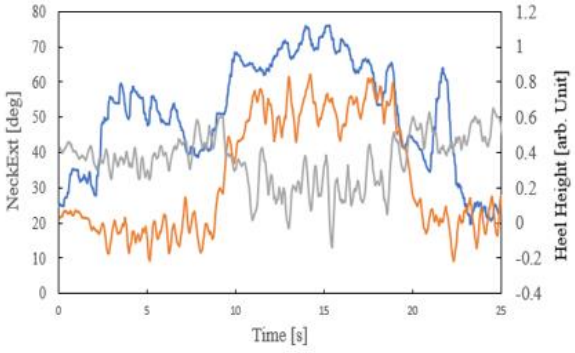

Figure 12. Results of the analysis when walking without aid.

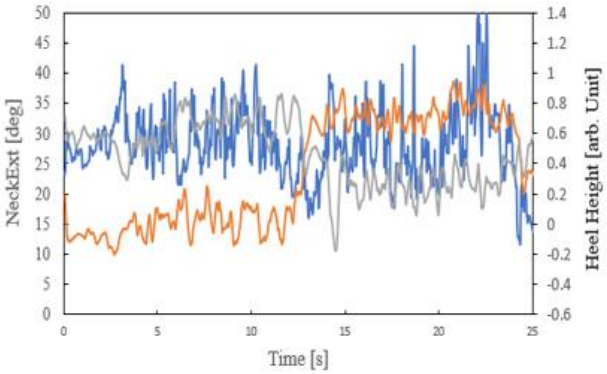

Figure 13. Results obtained when a walking aid was used.

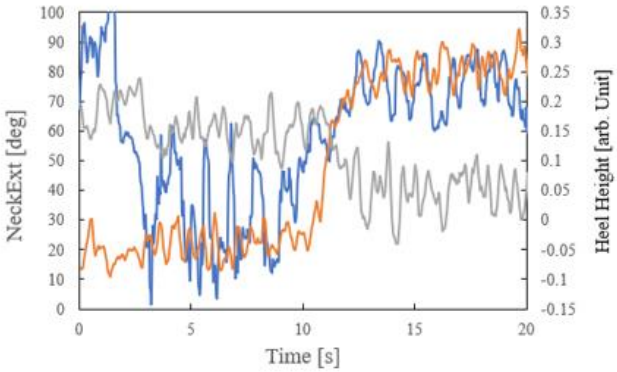

Figure 14. Results obtained approximately 5 min after using aid.

Figure 13 shows the results obtained when a walking aid was used. The tilt angle of the neck is also indicated by the blue line.

Figure 14 shows the measurement taken approximately 5 min after the aids were removed. This is a short time measurement because MediaPipe could not continuously capture the arm movements during this measurement, and the data stopped at 20 s.

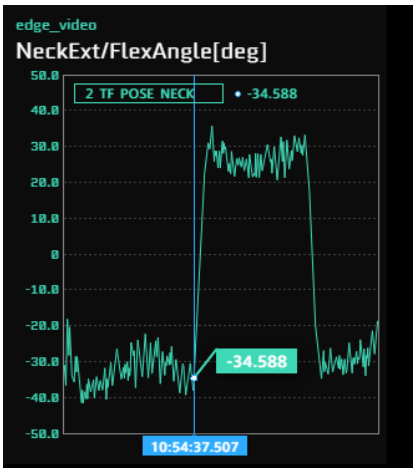

Figure 15. Change in neck tilt obtained using ORPHE ANALYTICS.

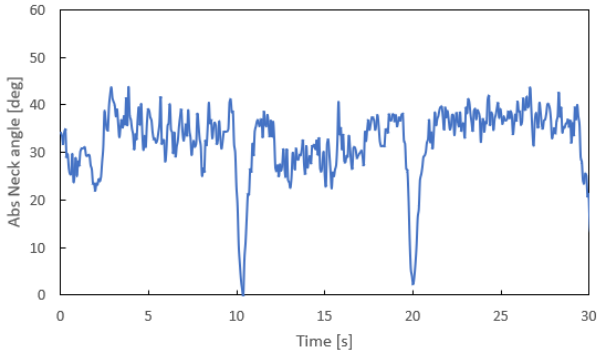

Figure 16. Absolute values of neck tilt before Orthobot use.

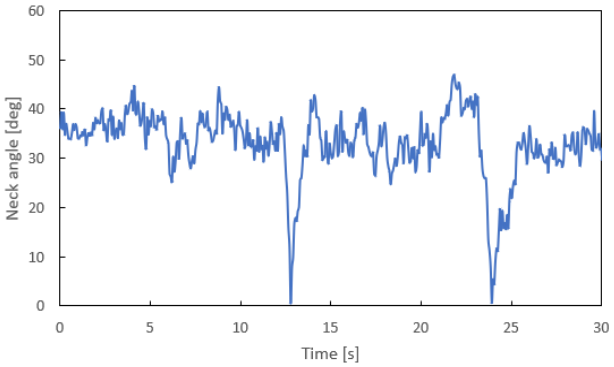

Figure 17. Absolute values of neck tilt during Orthobot use.

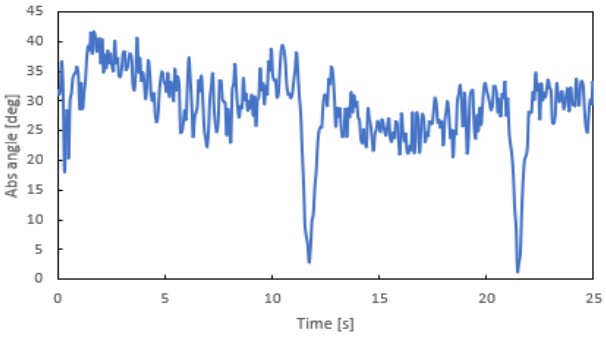

Figure 18. Absolute values of neck tilt 5 min after Orthobot use.

Figure 15 shows the change in the neck tilt obtained using the ORPHE ANALYTICS. This measurement was performed before the use of the Orthobot.

Figure 16 plots the absolute values for comparison with MediaPipe. This measurement was also conducted before the use of the Orthobot. Figure 17 shows the tilt of the neck while using the Orthobot. Figure 18 shows the measured neck tilt approximately 5 min after using the Orthobot. In Figure 16, the high-frequency signal with a relatively small amplitude is superimposed on the low-frequency signal as in the calculation with MediaPipe. For assisted aids, the high frequencies with large amplitudes have a noticeable number component. This trend is also observed in Figure 18, which

shows results of approximately 5 min after the supplementation with the Orthobot, with large amplitude high-frequency components.

G Discrete Fourier-transformation analysis for stride variability

The risk of falling is closely related to stride variability. Therefore, we focused on the variability and examined the frequency intensity using discrete Fourier-transformation (DFT) analysis. Figures 19-22 show the analysis results from the MediaPipe software, and Figures 23-25 show those from the ORPHE ANALYTICS. The DFT spectra were measured before, during, and 5 min after wearing the Orthobot walking assist device. Only 22 s of signal were used for the DFT evaluation, until the MediaPipe lost sight of a landmark point and stopped working properly when measured 5 min after removing the Orthobot.

The spectra of the neck angle changes before, during, and after using the assistive device obtained from ORPHE ANALYTICS are shown in Figures 23-25, with large peaks obtained in the low-frequency region below 0.5 Hz. The low-frequency peaks were particularly strong in the case of Figure 23 without the assistive device. The peak at approximately 1.6

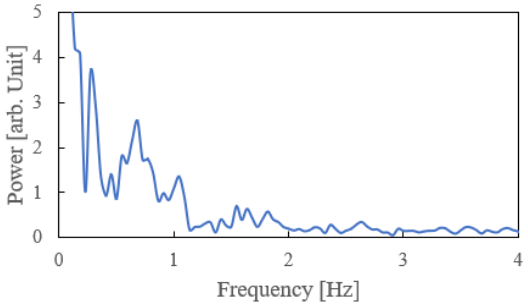

Figure 19. Spectrum before using Orthobot.

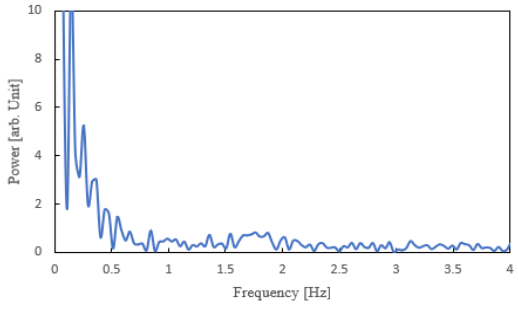

Figure 20. Spectrum when using Orthobot.

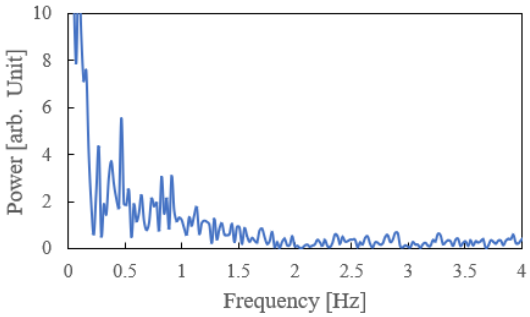

Figure 21. Spectrum after using Orthobot

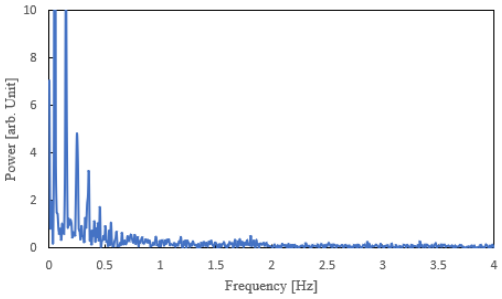

Figure 22. Sepctrum of heel using Orthobot.

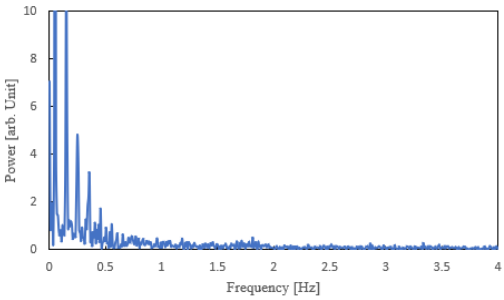

Figure 23. Spectrum before using Orthobot analyzed data obtained by ORPHE ANALYTICS.

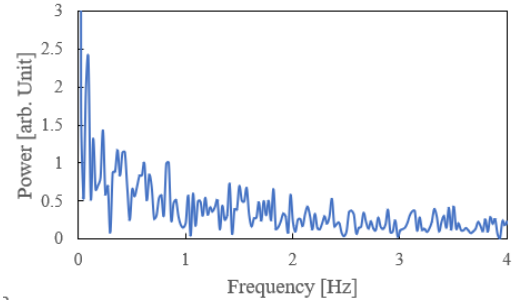

Figure 24. Spectrum when using Orthobot analyzed data obtained by ORPHE ANALYTICS.

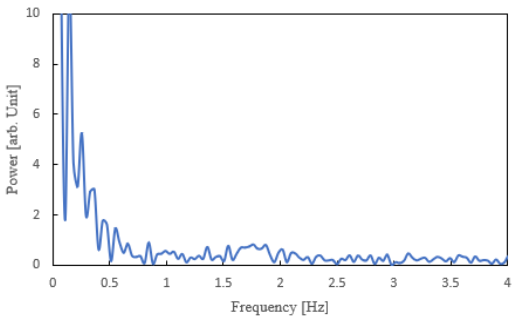

Figure 25. Spectrum of heel using the Orthobot analyzed data obtained by ORPHE ANALYTICS.

Hz decreased after the use of the assistive device, which may be due to the characteristics of the subject's gait.

III. DISCUSSION

A *Accuracy check of CSV data outputed by MediaPipe*

The analysis using MediaPipe reproduced the left ankle trajectory in the timed up-and-go measurements, as shown in Figure 2. The z-axis values corresponding to the vertical motion are small owing to the screen settings; therefore, the z-axis values are emphasized. Consequently, it is necessary to make a prior reference measurement and correction for an accurate evaluation. Detailed ankle trajectories were obtained. Video analysis of the timed up-and-go test confirmed that the specifications remained consistent.

B *Skeleton analysis of without/with restrictions using video from front and oblique upward angle*

As shown in Figures 4 and 6, it was possible to determine the ankle angle as gait condition data, although we did not calculate this timed up-and-go measurement. Comparing the independently measured range-of-motion angle data of the ankle joint and comparative ankle joint range-of-motion angles obtained from the video, slight differences were observed owing to the camera angles. The angular change in the right foot was almost the same, regardless of the camera angle. In contrast, the angular change in the left leg tended to be smaller. For the subject's gait, another measurement showed that the joint change in the left foot was smaller than that in the right foot. Further investigation is required in another experiment with a different subject.

C *Gait speed*

We considered the parts of the image that were considered to move as slightly as possible on the screen. In this image, the shoulders were close to the center of the image, so this was considered. In the walking speeds obtained by walking on the mat, differences of approximately 2.1 km/h and 1.3 km/h were obtained with and without the motion restriction, respectively. The values obtained from MediaPipe, however, were approximately an order of magnitude lower.

Although it is desirable to correct the coordinates from a three-dimensional perspective, in this case, the correction was based on the gait trajectory. Therefore, we compared the walking speeds based on measurements with known specific lengths. We examined the points that could be analyzed to obtain accurate results based on software principles. We inferred that it would be difficult to determine the gait speed when shooting from an oblique direction because the screen is moved in an oblique direction. However, we believe that, under the same conditions, we could obtain data for comparison. Obviously, the images taken from the front had a problem in that the size of the subject differed from one measurement data point to another.

Figure 8 shows a three-dimensional display of the trajectory of the right shoulder position. Because the slope of the change in the right shoulder position is approximately 45°, it was found that using the correction value for the direction of motion on the screen, a walking speed of 1.4 km/h was obtained, which was almost the same as the 1.3 km/h obtained from the mat.

Because the walking speed can be corrected by the choice of the detection point, it is necessary to be creative when capturing videos, for example, by shooting parallel to the direction of motion.

D *Tilt angle of neck calculated by Mediapipe and ORPHE ANALYTICS*

As shown in Figure 12, the tilt angle of the neck, indicated by the blue line, does not show a gradual change compared to the case without the aid, and a higher-frequency component can be observed. The change in the heel shape corresponded to the change in the vertical movement of the heel.

As shown in Figure 13, the tilt angle of the neck does not exhibit a gradual change compared with the case without the aid. A higher-frequency component can be observed in the change in the shape of the heel corresponding to the vertical movement of the heel.

Figure 14 shows a measurement taken approximately 5 min after the aids were removed. Although long-period waves were observed, high-frequency waves corresponding to the same up-and-down heel movements as when the assistive device was used were also observed, suggesting that the effect of the assistive device was still present.

In Figure 16, a high-frequency signal of a relatively small amplitude is superimposed on a low-frequency signal, as in the calculations with MediaPipe. In the assisted case, high species with large amplitudes have a noticeable number of components. This trend is also observed in Figure 19, which shows approximately 5 min after Orthobot replenishment and includes a high-frequency component of a large amplitude.

E DFT analysis for stride variability

In the spectrum before mounting shown in Figure 19, the peak change was gradual, as observed in the waveform, and the peak spectra were observed at 0.3, 0.6, and approximately 1 Hz. A small peak was also observed at approximately 1.7 Hz. Many fine peaks were observed in the knee joint flexion and extension movements when the subject wore the walking assist device because of the assisted movement. A peak at approximately 0.8 Hz was observed, although it was not a clear peak compared to the peak before the assist device was attached. A peak at approximately 1.6 Hz was also observed. Five minutes after the assist device was removed, not only a peak at approximately 0.8 Hz but also 0.9 Hz was observed, whereas a peak at approximately 1.6 Hz was observed; however, its amplitude was smaller. Figure 22 shows the results of the spectral analysis of the right heel of the right foot while wearing the assistive device, with peaks at approximately 0.4 Hz and 0.8 Hz. This suggests that these two peaks were caused by leg motion.

F Advantages and disadvantages of software implementation

Because this software can be installed on tablets and smartphones, we believe that the skeleton analysis screen can be effective as a simple check tool at rehabilitation sites. In the case of a detailed numerical analysis, there are differences in the numerical values obtained owing to differences in the camera angles, necessitating the use of a camera with a sufficiently wide angle at the time of measurement or having the camera fixed to eliminate shaking of the camera during movement. The current experiment only shows the results of the analysis of one subject with and without pseudo limitations of movement. Data from two subjects of different ages and genders measured simultaneously are currently being analyzed. Based on the above, we believe that the conditions necessary for using this software in the field can be determined by accumulating more data and adapting it to subjects with gait disorders.

IV. CONCLUSION AND FUTURE WORK

With the widespread use of smartphones, it is very easy to record videos of a person's walking condition and to ask for a diagnosis from a medical professional. The ability to obtain skeletal displays and numerical data, similar to this software, is expected to rapidly improve the potential of video analysis in the medical insurance field.

However, the limitations of shooting conditions when introducing this software should be considered. For example, the shooting angle and location on which the analysis should be focused are important. In the future, we will improve the optimization of the video shooting conditions and correction methods for all shooting angles. In addition, these corrections will be made and adapted for each subject.

We compared the foot movements of the Orthobot, an assistive device, before, during, and after 5 min of using MediaPipe and ORPHE ANYTICS. It was deduced that MediaPipe could obtain data over a considerable area. However, there are many areas where it is difficult to obtain the desired data through programming and to interpret the data; therefore, it is necessary to clarify the purpose of data collection for use in the field.

ACKNOWLEDGMENT

This work was supported by JAPS KAKENHI (grant number JP20K11924).

REFERENCES

[1] Y. Uchida, T. Funayama, Y. Kogure, "Investigation of the Application of MediaPipe to Gait Analysis," pp. 1-6, IARIA, GLOBAL HEALTH 2022. ISBN: 978-1-61208-995-9.

[2] L. G-Villanueva, S. Cagnoni, and L. Ascari, "Design of a Wearable Sensing System for Human Motion Monitoring in Physical Rehabilitation," Sensors, vol. 13, pp. 7735-7755, 2013.

[3] Y.-L. Zheng, X.-R. Ding, C. C. Y. Poon, B. P. L. Lo, H. Zhanf, and G-Z. Yang, "Unobtrusive Sensing and Wearable Devices for Health Informatics," IEEE Transactions Biomedical Engineering, vol. 61, pp. 1538-1554, 2014.

[4] M. M. Alam and E. B. Hamida, "Surveying Wearable Human Assitive Technology for the Life and Safty Critical Applocations: Standards, Challenges and Opportunities," Sensors, pp. 9153-9209, 2014.

[5] M. J. Deen, "Information and Communications Technologies for Elderly Ubiquitous Healthcare in a Smart Home," Personal and Ubiquitous Computing, pp. 573-599, 2015.

[6] S. Hong and K. S. Park, " Unobtrusive Photoplethymographic Monitoring Under the Foot Sole while in a Standing Posture," Sensors, 3239, 2018.

[7] V. Bucinskas, et al., "Wearable Feet Pressure Sensor for Human Gait and Falling Diagnosis," Sensors, vol. 21, 5240, 2021.

[8] P. M. Riek, A. N. Best, and R. Wu, "Validation of Inertial Sensors to Evaluate Gait Stability," Sensors, vol. 23, 1547, 2023.

[9] Y. Uchida et al., "Feature Value Extraction for Body Condition Change Measurement System Using Pressure Sensor Array," Human Interface Society in Japanese, vol. 24, No.1, pp. 79-82, 2022, ISSN 2188-6652.

[10] Y. Uchida, T. Funayama, K. Hori, M. Yuge, N. Shinozuka and Y. Kogure, "Possibility of Detecting Changes in Health Conditions using an Improved 2D Array Sensor System," Sensors & Transducers, vol. 259, pp. 29-36, 2022.

[11] Q. Zou, Y. Wang, Q. Wang, Y. Zhao, and Q. Li, "Deep Learning-Based gait Recognition Using Smartphones in the Wild," IEEE Transactions on Information Forensics and Security, pp. 1-15, 2020, arXiv:1811.00338v3 [cs.LG].

[12] F. Wang, A. Dong, K. Zhang, D. Qian, and Y. Tian, "A qualitative Assessment Grading Study of Balance Performance Based on Lowe Limb Dataset," Sensors, vol. 23, 33, 2023.

[13] V. Bazarevsky et al., " BlazePose: On-device Real-time Body Pose tracking," arXiv:2006.10204v1 [cs.CV] 2020.

[14] G. Kaur, G. Jaju, D. Agawal, K. Lyer, and C. M. Prashanth, "Implementation of Geriatric Agility Detection Using MediaPipe Pose," International Journal of Recent Advances in Multidisciplinary Topics, vol. 3, 119, 2022, ISSN:2582-7839.

[15] J.-L. Vhung, L.-Y. Ong, and M-C. Leow, "Comparative Analysis of Skelton-Based Human Pose Estimation," Future Internet, vol.14, 380, 2022.

[16] J.-W, Kim, J.-Y. Choi, E.-J. Ha, and J.-H. Choi, "Human Pose Estimation Using MediaPipe Pose and Optimization Method Based on Humanoid Model," Applied Sciences, vol. 12, 2700, 2023. doi.org/10.3390/app13042700.

[17] Q. Wang, g. Kurilo, F. Ofli, and R. Bajcsy, "Evaluation of Pose tracking Accuracy in the First and Second Generations of Microsoft Kinect," arViv:1515.04134v1 [cs.CV] 2015.

[18] P. Plantard, E. Auvinet, A. S. Le Pierres, and F. Multon,"Pose Estimation with a Kinect for Ergonomic Stuidies: Evaluation of the Accuracy Using a Virtual Mannequin," Sensors, vol. 15, pp. 1785-1803, 2015.

[19] R. A. Clark, B. F. Mentiplay, E. Hough, and Y. H. Pus, "Three-Dimensional Cameras and Skeleton Pose Tracking for Physical Function Assessment: A Review of Use, Validity, Current Developments and Kinect Alternatives," Gait & Postture, vol. 68, pp. 193-200, 2019.

[20] Y. Ma, K. Mithratatne, N. Wilson, Y. Zhang, and X. Wang, "Kinect v2-Based Gait Analysis for Children with Cerebral Palsy: Validity and Reliability of Spaial Margin of Stability ad Spationtemporal Vaiables," Sensors, vol. 21, 2104, 2021.

[21] D. Imoto, S. Hirano, M. Mukaino, E. Saitoh, and Y. Otaka, "A Novel Gait Analysis System for Detecting Abnormal Hemiparetic Gait Patterns during Robo-assisted Gait Training : A Criterion Validity Study among Healthy Adults," Frontiers in Neurorobotics, 16:1047376, 2022.

[22] L. Buker, V. Quinten, M. Hackbarth, S. Hellmers, R. Diekmann, and A. Hein, "How the Processing Mode Influences Azure Kinect Body Tracking Results," Sensors, vol. 23, 878, 2023.

[23] K. Shihomi, K. Ohata, T. Tsuboyama, Y. Sawada, and Y. Higashi, "Development of New Rehabilitation Robot Device that Can be Attached to the Conventional Knee-Ankle-Foot-Orthosis for Controlling the Knee in Individuals After Stroke," 2017 International Conference on Rehabilitation Robotics, pp. 304-307, 2017.

[24] A. L. Hof, M. G. J. Gazendam, and W. E. Sinke, "the condition for dynamic stability," Journal of Biomechanics, vol. 38, pp. 1-8, 2005.

[25] R. M. Magnani, S. M. Bruijn, J. van Dieen, and M. F. Vieira, "Head Orientation and Gait Stability in Young Adults, Dancers and Older Adults," Gait & Posture, vol. 80, pp. 68-73, 2020.

[26] J. Choi, S. M. Parker, Y. Gwon, and J. Youn, "Wearable Sensor-Based Prediction Model of Time up and Go Test in Older Adults," Sensors, vol. 21, 6831, 2021.

[27] J. Beyea, C.A. McGibon, A. Sexton, J. Noble, and C. O'Connell, "Covergent Validity of a Wearable Sensors Sytem for Measuring Sub-Task Performance during the Timed Up-and-Go test," Sensors, vol. 17, 934, 2017.

[28] J. P. Monteiro, A. T. Magalhaes, and H. P. Oliveira, "Human Pose Estimation, Anthropomorphism and Gamification in Promotion of Physical Activity Among Breast Cancer Surviviors," International Journal on Advances in Life Sciences, vol. 11, pp. 118-127, 2019.

[29] F. Buisseret et al., "Time Up and Go and Six-Minute Walking Test with Wearable Inertial Sensor: One Step Futher for Prediction of the Risk of Fall in Elderly Nursing Home People," Sensors, vol. 20, 3207, 2020.

[30] A. L. M. Frangakis, E. D. Lemaire, and N. Baddour, "Subtask Segmentation Method of the Timed Up and Go test and L Test Using Inertial Measurement Units-A Scoping Review," Information, vol. 14, 127, 2023.

[31] Z. Li, R. Zhang, C. H. Lee, and Y. Lee, "An Evaluation of Posture Recognition Based on Intelligenct Rapid Entire Body Assessment System for Determing Musculoskeletal Disorders," Sensors, vol. 20, 4414, 2020.

[32] Y. Ono, O. D. A. Prima, and K. Hosogoe, "Evaluation and Application of Partial Body Joint Model in 3D Human Pose Estimation from Signal Image," International Journal on Advances in Life Sciences, vol. 13, pp. 114-123, 2021.

[33] I. Crombrugg et al., "Accuracy Assessment of Joint Angles Estimated from 2D and 3D Camera Measurements," Sensors, vol. 22, 1729, 2022.

[34] X. Yu, J. Baar, and S. Chen, "Joint 3D Human Shape Recovery and Pose Estimation from a Signal Image with Bilayer Graph," arXiv:2110.8472v2 [cs.CV], 2021.